ACCOUNTS of chemical research

pubs.acs.org/accounts Article

Vanadium-Based Materials: Next Generation Electrodes Powering the Battery Revolution?

Shipeng Zhang,[⊥] Huiteng Tan,[⊥] Xianhong Rui,* and Yan Yu*

Cite This: https://dx.doi.org/10.1021/acs.accounts.0c00362 Read Online

ACCESS | Metrics & More | Article Recommendations

CONSPECTUS: As the world transitions away from fossil fuels, energy storage, especially rechargeable batteries, could have a big role to play. Though rechargeable batteries have dramatically changed the energy landscape, their performance metrics still need to be further enhanced to keep pace with the changing consumer preferences along with the increasing demands from the market. For the most part, advances in battery technology rely on the continuing development of materials science, where the development of high-performance electrode materials helps to expand the world of battery innovation by pushing the limits of performance of existing batteries. This is where vanadium-based compounds (V-compounds) with intriguing properties can fit in to fill the gap of the current battery technologies.

The history of experimenting with V-compounds (i.e., vanadium oxides, vanadates, vanadium-based NASICON) in various battery systems, ranging from monovalent-ion to multivalent-ion batteries, stretches back decades. They are fascinating materials that display rich redox chemistry arising from multiple valency and coordination geometries. Over the years, researchers have made use of the inherent ability of vanadium that undergoes metamorphosis between different coordination polyhedra accompanied by transitions in the oxidation state for reversible intercalation/insertion of more than one guest ions without breaking the structure apart. Such infinitely variable properties endow them with a wide range of electronic and crystallographic structures. The former attribute varies from insulators to metallic conductors while the latter feature gives rise to layered structures or 3D open tunnel frameworks that allow facile movement of a wide range of metal cations and guest species along the gallery. Accompanied by a growing stringent requirements for energy storage applications, most V-compounds face difficulty in resolving the problems of their own lack competitiveness mostly due to their intrinsically low ionic/electronic conductivity. The key to producing vanadium-based electrodes with the desired performance characteristics is the ability to fabricate and optimize them consistently to realize certain specifications through effective engineering strategies for property modulation.

In this Account, we aim to provide a comprehensive article that correlates the fundamental of charge storage mechanism to crystallographic forms and design principle for V-compounds. More importantly, the essential roles played by engineering strategies in the property modulation of V-compounds are pinpointed to further explain the rationale behind their anomalous behavior. Apart from that, we further summarize the key theoretical and experimental results of some representative examples for tuning of properties. On the other hand, advances in characterization techniques are now sufficiently mature that they can be relied upon to understand the reaction mechanism of V-compounds by tracing real-time transformation and structural changes at the atomic scale during their working state. The mechanistic insights covered in this Account could be used as a fundamental guidance for several key strategies in electrode materials design in terms of dimension, morphology, composition, and architecture that govern the rate and degree of chemical reaction.

KEY REFERENCES

- Rui, X.; Sun, W.; Wu, C.; Yu, Y.; Yan, Q. An Advanced Sodium-Ion Battery Composed of Carbon Coated $Na_3V_2(PO_4)_3$ in a Porous Graphene Network. *Adv. Mater.* **2015**, *27*, 6670−6676.[1] *3D porous $Na_3V_2(PO_4)_3$-based cathode with bicontinuous ion/electron pathways and large electrode−electrolyte contact area exhibited an ultralong-life cycling stability at 100 C.*
- Chen, D.; Rui, X.; Zhang, Q.; Geng, H.; Gan, L.; Zhang, W.; Li, C.; Huang, S.; Yu, Y. Persistent Zinc-Ion Storage in Mass-Produced V_2O_5 Architectures. *Nano Energy* **2019** *60*, 171−178.[2] *A facile strategy was developed to fabricate V_2O_5 nanorods-constructed 3D porous architectures in kilogram scale, which showed the enhanced zinc*

Received: June 8, 2020

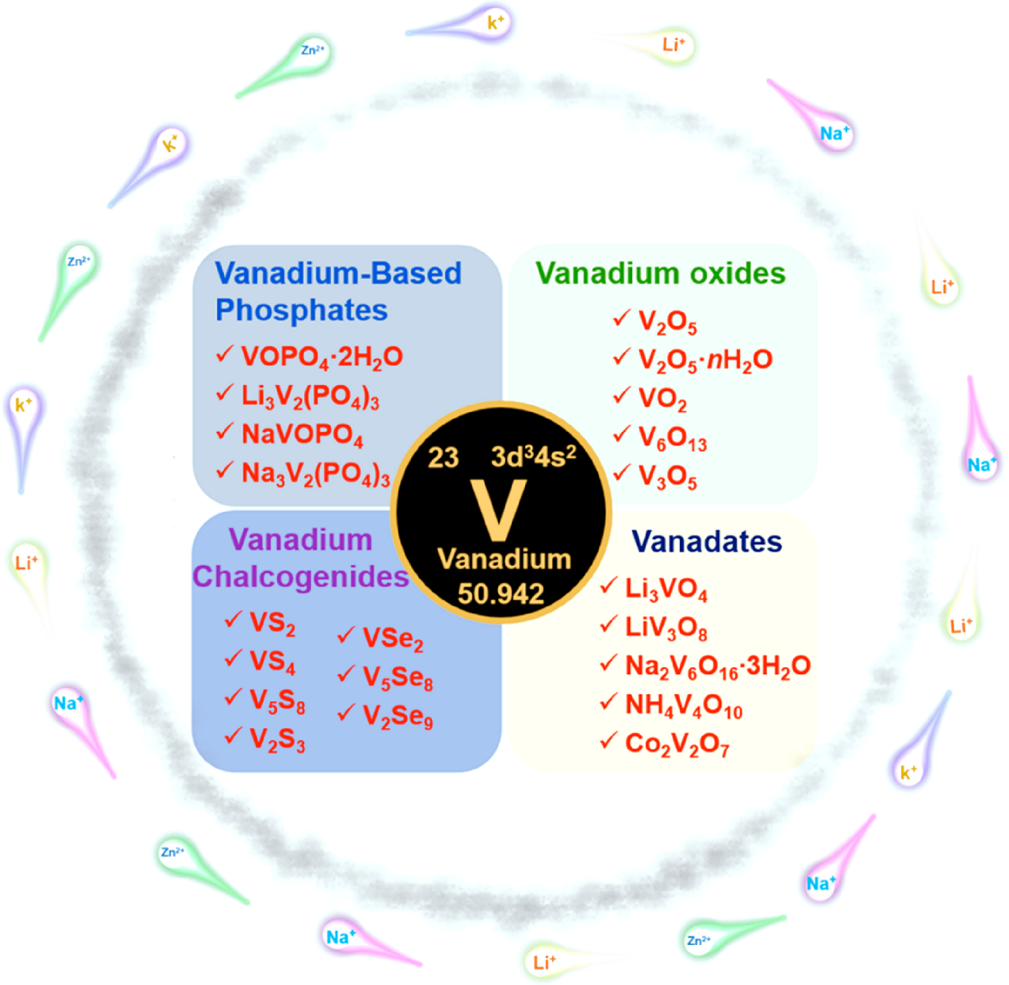

Figure 1. V-compounds with multielectron redox reactions for rechargeable batteries.

storage performances (e.g., outstanding long-term cyclic stability at 10 A g^{-1} for 5000 cycles).

- Shen, L.; Chen, S.; Maier, J.; Yu, Y. Carbon-Coated Li_3VO_4 Spheres as Constituents of an Advanced Anode Material for High-Rate Long-Life Lithium-Ion Batteries. *Adv. Mater.* **2017**, *29*, 1701571.[3] *A high-performance full lithium-ion battery that fabricated using carbon-coated Li_3VO_4 spheres showed an estimated practical energy density of 205 Wh kg^{-1} with greatly improved long-term cyclability and rate capability.*
- Ding, Y.-L.; Wen, Y.; Wu, C.; van Aken, P. A.; Maier, J.; Yu, Y. 3D V_6O_{13} Nanotextiles Assembled from Interconnected Nanogrooves as Cathode Materials for High-Energy Lithium Ion Batteries. *Nano Lett.* **2015**, *15*, 1388−1394. *3D V_6O_{13} nanotextiles built from interconnected 1D nanogrooves were fabricated at room temperature as high energy cathode for lithium-ion batteries.*

1. INTRODUCTION

The future global economy will put unprecedented strain on energy demands under the burden of a rising population that consumes the limited resources in the earth. Electrochemical energy storage, especially rechargeable batteries, has been one of the potential solutions put forward. Over the years, commercial rechargeable batteries have widely penetrated the stationary, portable, and transportation markets by offering a perfect combination of energy/volume density (100−300 Wh kg^{-1}/250−650 Wh L^{-1}), longevity, and affordability. While batteries have laid the foundation for a fossil fuel-free society, building the battery of the future necessitates a new wave of chemistries that are capable of pushing the boundaries of current performances.

During our journey working on new battery materials with appealing capacity and energy density, we settled on V-compounds, as they display a wide range of electronic and crystallographic structures arising from the great stability of various oxidation states (from +5 to +2) and coordination environments (Figure 1). For example, V_2O_5 is known for its multielectron transition that can deliver a high theoretical capacity of 294 mAh g^{-1} with 2 Li^+ (de)intercalation. The highly covalent 3D structure of vanadium phosphates provides enhanced structural and thermal stability even at high charge states. In addition, the inherently high ionic conductivity of $Li_3V_2(PO_4)_3$ (LVP) and $Na_3V_2(PO_4)_3$ (NVP) allows cations to diffuse through their interstitial spaces facilely at high average operating voltage of 4.0 V (vs Li/Li^+) and 3.4 V (vs Na/Na^+) respectively (diffusion coefficient: 10^{-9}−10^{-10} and ~10^{-14} cm^2 s^{-1} for LVP and NVP, respectively). Apart from that, Li_3VO_4 is an insertion-type anode with high ionic conductivity (~10^{-8} S cm^{-1} at room temperature) at a relatively low voltage range between 0.2 and 1.0 V vs Li/Li^+, which can potentially replace the role formerly reserved by

https://dx.doi.org/10.1021/acs.accounts.0c00362
Acc. Chem. Res. XXXX, XXX, XXX−XXX

graphite and $Li_4Ti_5O_{12}$. Nevertheless, the challenges in developing high-performance V-compounds lie in the slow reaction kinetics that arise from their low electronic conductivity. The deficiency of being less electronically reactive poses a significant barrier for V-compounds to fully claim their theoretical energy and power density. Another major issue of V-compounds is associated with the amphiprotic nature of vanadium, where deleterious interfacial reaction between the electrolyte (strong Lewis acid) and vanadium through acid−base interaction exacerbates its dissolution problem.[5] As a result, the catalytic decomposition of the electrolyte can trigger rapid capacity fading due to the loss of active materials. The moderate toxicity of vanadium is one of the concerns that should not be overlooked. It is generally known that the toxicity of vanadium varies with its physicochemical state, where it increases, as a rule, with valence. Despite their great promise, effective engineering strategies are highly sought after to tailor the intrinsic disadvantages of V-compounds.

In this Account, we aim to provide a holistic snapshot of the development of V-compounds that correlates the fundamentals of the charge storage mechanism to the design principle of V-compounds. More importantly, we hope to pinpoint the essential role played by engineering strategies in the properties modulation of V-compounds. On top of that, a balanced and facts-based perspective is provided to elucidate the promise and current status of V-compounds, which is helpful in devising strategies for the future batteries.

2. ELECTROCHEMICAL THERMODYNAMICS AND KINETICS OF VANADIUM-BASED ELECTRODES

Thermodynamically, the Nernst equation can also be translated into an expression where the difference in Li chemical potentials (μ_{Li}) between the anode and cathode determines the cell voltage:[6]

$$V_{OC} = \frac{(\mu_{Li}^{cathode} - \mu_{Li}^{anode})}{n} \quad (1)$$

Taking the lithium ion battery (LIB) as an example where the Li reference anode remains a constant value in chemical potential, the chemical potential of interstitial Li in an intercalation compound can be expressed as the derivative of the free energy of the material with respect to Li concentration (x):[7]

$$\mu_{Li} = \frac{\partial G}{\partial x} \quad (2)$$

Graphically, the μ_{Li} within the intercalation V-compounds can be derived from the slope of the free energy at a particular composition, which establishes a straightforward connection between a measurable voltage curve and the nature of phase transformations with respect to the variations in Li concentration. For example, a single-phase solid solution reaction of LVP gives rise to a smoothly sloping voltage curve.[8] In contrast, a first-order phase transformation from a Li-poor phase α to a Li-rich phase β leads to a plateau voltage profile in the phase separation region.[7] Steps shown in the voltage curve are indicative of a phase separation reaction, where a stable intermediate with lower Gibbs free energy is likely to form over the energetically favorable phase. Our recent research focused on nanosized V-compounds has shown a deviation in the shape of the voltage curve arising from their difference in the chemical potential along various crystal orientations near the surface due to a change in Gibbs free energy caused by high surface or interface energy. Therefore, a sloping voltage profile is more likely to be observed as the miscibility gap between two local minima is significantly reduced with the additional free energy.[9,10]

The thermodynamics expression signifies the large available energy in cells based on the V-compounds at equilibrium condition. However, their theoretical value of chemical energy can seldom be fully claimed due to the presence of overpotential caused by kinetic limitations of the complicated reaction environment. In summary, overpotential (η) is recognized to be the total voltage drop-off induced by activation polarization, concentration polarization and ohmic polarization:[11]

$$\eta = V_{oc} - V_t \quad (3)$$

$$\eta = [(\eta_{act})_a + (\eta_{act})_c] - [(\eta_{conc})_a + (\eta_{conc})_c] + IR \quad (4)$$

V_{oc} and V_t are the open circuit voltage and terminal cell voltage respectively, $(\eta_{act})_a$ and $(\eta_{act})_c$ are the activation polarization at the anode and cathode,respectively, $(\eta_{conc})_a$ and $(\eta_{conc})_c$ are the concentration polarization at the anode and cathode respectively, I is the load current, and R is the internal resistance of the cell.

The activation polarization is the voltage drop arising from the charge transfer reaction at the electrode/electrolyte interfaces, which can be described using the Butler−Volmer equation to illustrate how the current flow (i) varies with overpotential:[12]

$$i = i_0 \exp\left(\frac{\alpha F\eta}{RT}\right) - \exp\left[\frac{(1-\alpha)F\eta}{RT}\right] \quad (5)$$

where $i_0 = K_0FA$ *is* the exchange current density, K_0 is the reaction rate constant, A is the activity of the reactants, α is the transfer coefficient, T is the temperature in Kelvin, and R is the gas constant. This kinetic hindrance involves the charge transfer at the electrode/electrolyte interfaces, in which the activation barrier on ion mobility within the V-compounds can be strategically minimized if a highly conductive interface for facile electron transfer is provided. The concentration polarization is tied with the rate of ion transportation from the bulk to the surface of the electrode materials:[11]

$$\eta_c = E_s - E_b = \left(\frac{RT}{nF}\right)\ln\left(\frac{C_s}{C_b}\right) \quad (6)$$

where η_c, E_s, E_b, C_s, and C_b are the concentration polarization, electrode potential at the surface, electrode potential in the bulk solution, concentration at the electrode surface and the concentration in the bulk solution. Previous findings associated with property modulation of V-compounds have hinted the possible ways to minimize the concentration polarization by continuously replenishing the electrolyte surface with incoming electrolyte ion from the bulk solution. Therefore, engineering strategies that can successfully address the mass transport issue would be helpful to provide a shorter ion transport pathway toward the V-compounds. The ohmic polarization (η_{ohm}) is associated with the resistances caused by various components of a battery, such as the electrolyte, current collector, additives, and contact between the active materials and the current collector. It is simplified as internal resistance as follows:[11]

https://dx.doi.org/10.1021/acs.accounts.0c00362
Acc. Chem. Res. XXXX, XXX, XXX−XXX

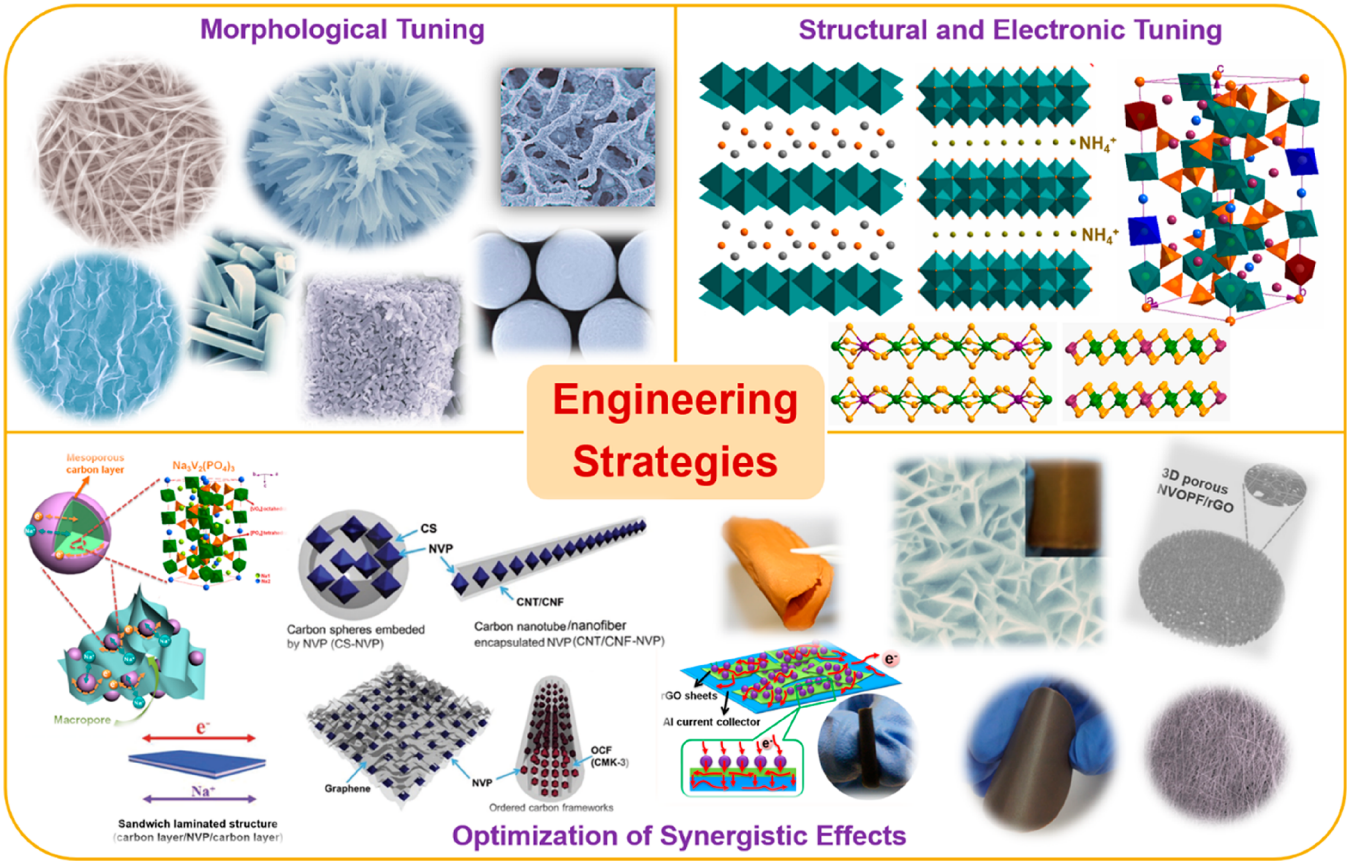

Figure 2. Summary of the common engineering strategies used to boost the electrochemical performances of vanadium-based electrodes.

$$\eta_{ohm} = IR \tag{7}$$

This is to say, a reduced overpotential can be obtained through the fabrication of self-supported vanadium-based electrodes without employing electro-inert binders.[13] The electron transfer process at the electrode/current collector interfaces is not retarded by the insulating binder or the long-range distance between the V-compounds and current collector, which is also beneficial for improving the power density of battery.

3. OPTIMIZATION AND DESIGN FOR VANADIUM-BASED ELECTRODES

The key to producing V-compounds with the desired performance characteristics is the ability to fabricate and optimize them consistently to realize certain specifications for battery applications. At a fundamental level, the engineering strategies that are effective for property modulation are summarized in Figure 2.

3.1. Morphological Tuning

The anomalous behavior of nanostructures can be rationalized by Fick's law ($\tau \propto \frac{L^2}{D}$), where a reduced diffusion length (L) confers to a shorter ion diffusion time (τ). This phenomenon confirms the fact that nanostructuring enables a higher influx of ion across the interface to accelerate the reaction of vanadium-based electrodes. In our attempt to grapple with the intrinsic limitations of V-compounds, the concept of morphological tuning in their nanoform was brought up, where the 0D, 1D, and 2D V-compounds nanostructures are those successful examples.[14−17] Furthermore, we found that the pseudocapacitive character of V-compounds is increasingly evident when their sizes fall into the nanoregime, which is beneficial for addressing the slow solid-state diffusion of intercalating ions.[2,10] Given that a large number of charges can be accumulated near the surface within microsecond to millisecond time scales, the reaction taking place in nanostructured electrodes entails significant suppression of intercalation induced phase transition, giving rise to better kinetics than that of the typical diffusion-controlled faradaic reaction.[18] Proceeding under this assumption, we can correlate the unprecedented rate capability to the increasing capacitive-controlled storage mechanism in nanostructured V-compounds. Rationally designing V-compounds into nanostructures might help, but a better way comes with the construction of a 3D secondary structure that can preserve the advantageous features of a certain morphology without compromising on the merits of the nanostructure. Our group recognized early that the limitation in mass transport at the interface can be mitigated by the morphological control of nanostructures. With the 3D porous secondary structure, the concentration polarization can be minimized with better electrolyte immersion. Furthermore, a higher reaction rate can be sustained through the 3D continuous electron/ion transport pathways via interconnected nanoscale building blocks and suppression of self-agglomeration and pulverization.[4,19,20]

3.2. Structural and Electronic Tuning

Kinetics studies have revealed the critical role of the lattice environment that changes the interaction between cation and host materials.[21] The introduction of a shielding hydrate layer or intercalation of alkali ions improves the kinetics of ion

https://dx.doi.org/10.1021/acs.accounts.0c00362
Acc. Chem. Res. XXXX, XXX, XXX−XXX

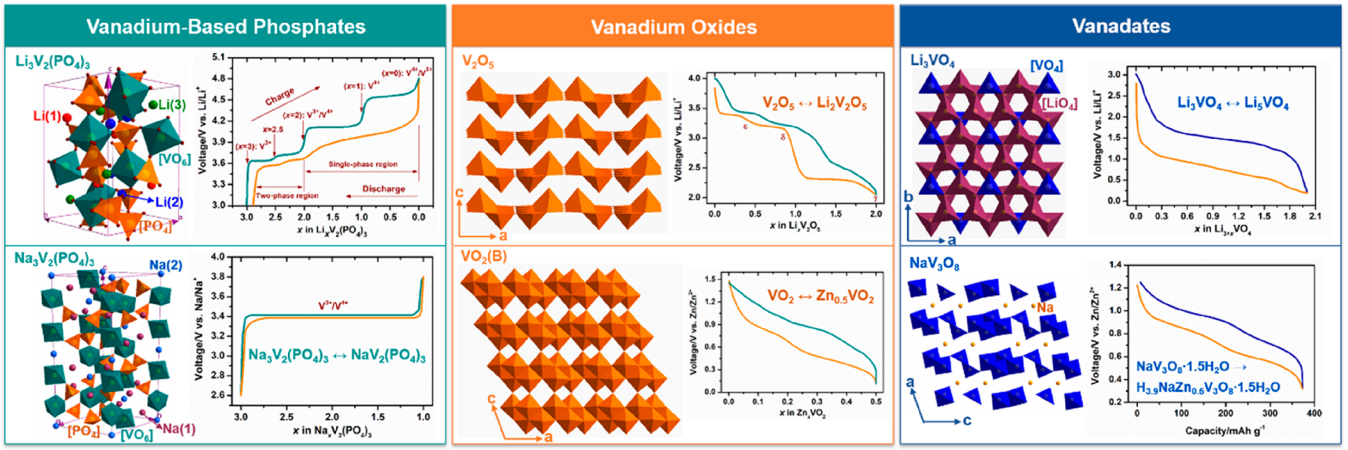

Figure 3. Summary of the electrochemical characteristic of the promising V-compounds.

migration by modulation of the polarity and dimension of the anion framework. In addition to being able to expand the interlayer spacing of layered V-compounds, structural water enhances the mobility of intercalating ions by shielding their charge, as a way to reduce the trapping force endorsed by lattice oxygen. On the other hand, the pillaring effect exerted by the preinserted species further stabilizes the interlayer structure, though their coordination might cause a shrinkage of the lattice beforehand. These concepts have been validated in our recent studies on vanadium-based electrodes.[22,23]

In addition, doping cations introduce defects, such as vacancies and holes, that counteract the imbalance of electrical neutrality in the crystal lattice.[24] Therefore, the electronic conductivity can be enhanced with the generation of hole. Given the correlation between ion diffusivity and activation energy represented in the classical Arrhenius equation: $D_i = D_0 \exp\left(-\frac{\Delta G}{k_B T}\right)$ (ΔG is the energy barrier, k_B is the Boltzmann constant, T is the temperature, and D_0 is the pre-exponential factor),[25] lattice engineering through ion doping and lattice expansion could also be the method of choice to tune the activation energy of V-compounds. In particular, the larger radius of alkaline ions (Na^+ and K^+) and higher charge of Zn^{2+} makes their intercalation more kinetically unfavorable, not to mention their sluggish migration in the lattice structure as compared with Li^+. A study reported by Cao and co-workers is particularly interesting as they revealed the central role of chemically inserted cations that enlarges the interlayer spacing by inducing the formation of V^{4+} species.[26] This concept is eventually generalized to other transition metals to tackle the sluggish insertion kinetics of intercalating ions, which provides insightful guidelines for the development of high-performance V-compounds.

3.3. Optimization of Synergistic Effects

Surface engineering improves the structural stability and conductivity by regulating the surface chemistry and chemical response. Conformal carbon coating is particularly common for V-compounds, as it offers multiple advantages in a readily achievable way by employing widely available carbon sources, such as polymers, polysaccharides, and organic acids.[27−29] The enhanced electrochemical performances can be explained from the following perspectives: (i) a conductive coating improves the electronic and ionic conductivity; (ii) mechanical confinement suppresses severe volume expansion; (iii) a buffer layer stabilizes the solid−electrolyte interface (SEI). Further research in our group was devoted to marrying the surface engineering with other strategies for greater impact. With all these delineations in mind, Yao et al. modified the strategy by making use of ionic liquid as the N-doped carbon source in the synthesis of NVP.[30] With a well-protected surface and improved electronic conductivity endowed by the N-doped carbon, the NVP composite exhibits remarkable performance in both long-term cycling and rate tests.

The synergistic coupling effect that is induced by the juxtaposition of disparate types of materials provides a viable solution to ameliorating the sluggish kinetics of electronic and ionic transport encountered by most V-compounds. Among various possible combinations, carbon-based scaffolds are able to provide highly compatible features with V-compounds to unleash their full potential. For example, V_2O_5,[31] LVP,[24] and NVP[32] tethered on the surface of carbonaceous materials have endowed them with enhanced electrochemical properties, which can be explained from the following aspects: (i) carbon supports with high conductivity facilitate efficient charge transfer; (ii) severe agglomeration can be prevented; (iii) confinement of carbon maintains the structural integrity of the V-compounds. Apart from that, what makes carbon a versatile support is its high tunability, where it can be transformed into several other forms after the introduction of defects and vacancies induced by doped or absent atoms. These findings have further sparked the investigation of chemically synthesized doped frameworks, biologically derived materials, and organics with intrinsic doping (e.g., polymers and ionic liquids) as conductive scaffolds. The modified carbon is endowed with enhanced surface wettability and favorable binding sites for cations. These unique properties, merged with the fact that carbon materials provide synergistic enhancement in electronic conductivity of the electrode, are a plausible explanation for the improved reaction kinetics.[33]

4. PROMISING VANADIUM-BASED ELECTRODES

The discussions in this section will be directed to our research on vanadium-based electrodes, with an emphasis on the correlation between engineering strategies and their charge storage properties. Their electrochemical characteristics are summarized in Figure 3 for comparison.

https://dx.doi.org/10.1021/acs.accounts.0c00362
Acc. Chem. Res. XXXX, XXX, XXX−XXX

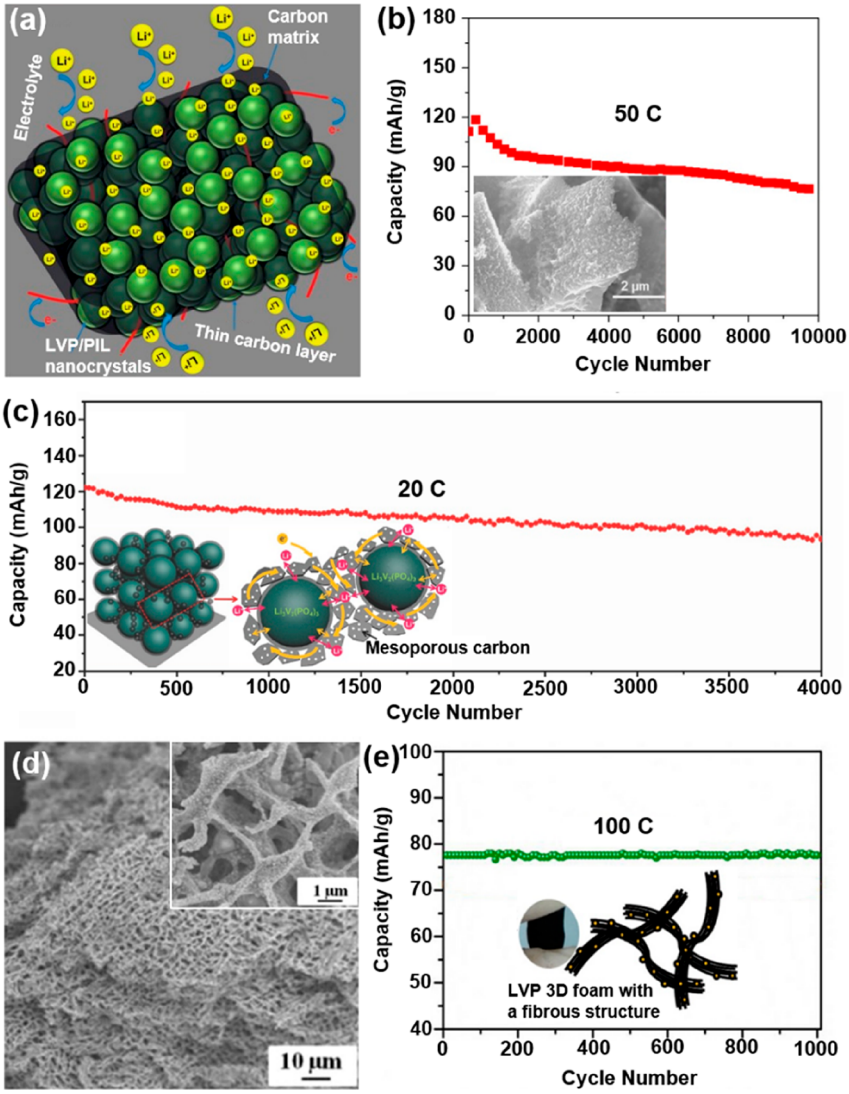

Figure 4. (a) Schematic representation of the Li^+ and electron pathways of the LVP/PIL and (b) the corresponding cycling performance (inset: SEM image). (a, b) Reproduced with permission from ref 35. Copyright 2015 Elsevier. (c) Long-term cycling of the LVP/C (inset: schematic illustration of the Li^+ and electron pathways). Reproduced with permission from ref 36. Copyright 2014 Wiley-VCH. (d) SEM images of the LVP 3D foam and (e) its cycling performance. (d, e) Reproduced with permission from ref 37. Copyright 2015 American Chemical Society.

4.1. Vanadium Phosphates

4.1.1. $Li_3V_2(PO_4)_3$. Despite the high theoretical capacity (197 mAh g^{-1} with 3 Li^+ insertion/extraction) of LVP, it is limited by the low electronic conductivity (2.4×10^{-7} S cm^{-1}).[24,34] In our initial work investigating the Li^+ diffusion rate of LVP, we discovered the voltage dependent diffusion behavior of LVP, where a phase transition region usually causes higher energy barriers for ion diffusion compared to the solid solution region. This basic insight about the nature of transformation on the electrochemistry of V-compounds has been an important guidance for future optimization of other intercalation compounds through structural engineering.[8] Moreover, the low electronic conductivity issue of LVP can be mitigated in the presence of carbon matrices, which can be either in encapsulation or deposition form, for enhanced charge transfer and stability. For example, the LVP/carbon composite reported by Balducci's group can sustain high cycling stability up to 10 000 cycles at a high rate of 50 C (Figure 4a,b).[35] Similarly, Mai et al.'s study that employed the same strategy focused more on the fabrication of LVP into 3D hierarchical carbon-decorated structures, which led to an insignificant capacity fading of 0.0065% per cycle at a high rate of 20 C after 4000 cycles (Figure 4c).[36] When the nanoporous carbon network was further modified into a 3D form via a bioinspired method in our previous study, the structural advantages have translated into a boost in several aspects of the performance. For example, the encapsulated LVP can be cycled up to 1000 cycles with almost no obvious capacity fading at 100 C (Figure 4d,e), along with a high energy density of 205 Wh kg^{-1} at a power density of 41 kW kg^{-1}.[37]

4.1.2. $Na_3V_2(PO_4)_3$. Similar to LVP, NASICON-type NVP has a promising theoretical capacity of 117 mAh g^{-1} (2 Na^+ insertion/extraction) but moderate electronic conductivity that is at only slightly higher value of 1.63×10^{-6} S cm^{-1}. A common strategy that helps to shorten the diffusion length of ion/electron would dictate compositing NVP with conductive matrices to afford better performance. In addition to the conventional wisdom that relies on in situ covalent hybridization of carbon-based materials with NVP, the impact of secondary structure was taken into consideration in our

https://dx.doi.org/10.1021/acs.accounts.0c00362
Acc. Chem. Res. XXXX, XXX, XXX−XXX

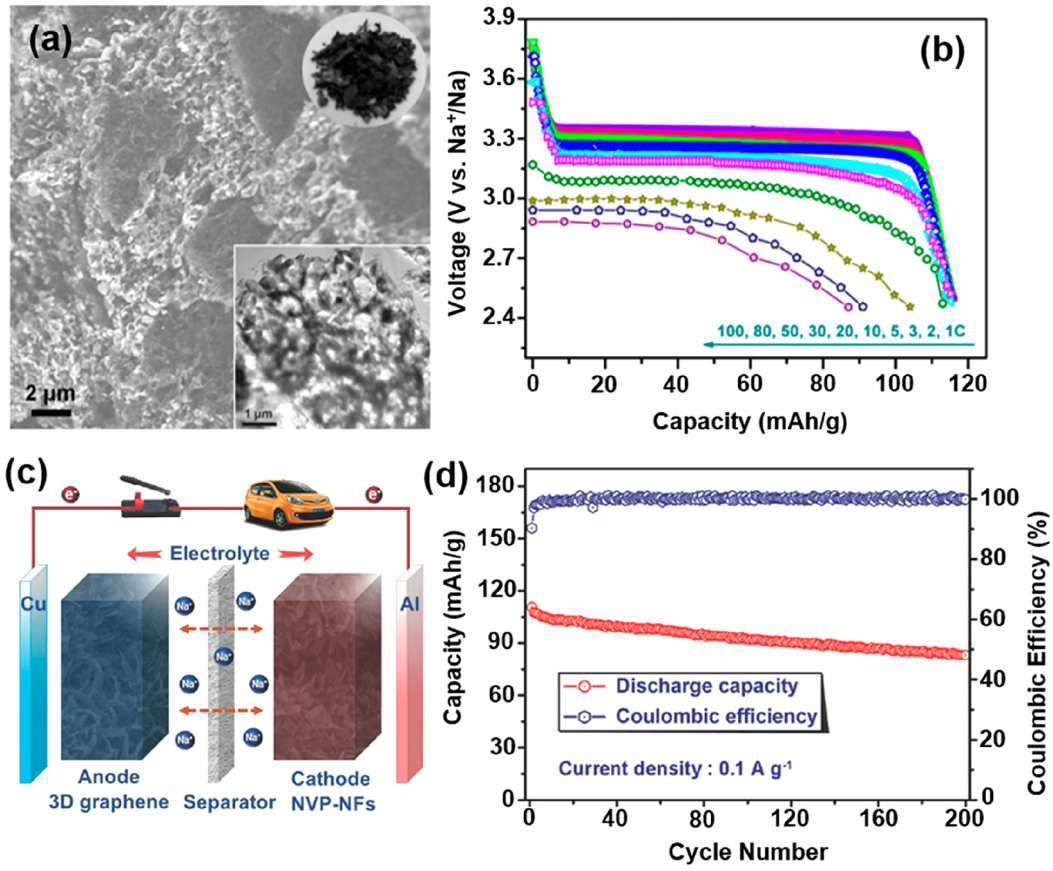

Figure 5. (a) SEM image of the NVP@C@rGO and (b) its discharge profiles at various current rates. (a, b) Reproduced with permission from ref 1. Copyright 2015 Wiley-VCH. (c) Schematic illustration and (d) cycling performance of the full cell based on 3D graphene-capped NVP. (c, d) Reproduced with permission from ref 39. Copyright 2017 Wiley-VCH.

previous studies to allow better accessibility of electrolyte and suppression of volume expansion.[38] For example, an extremely stable cycling performance of over 10 000 cycles at 100 C was delivered by the 3D hierarchical porous NVP-based hybrid (Figure 5a,b).[1] With the effect of doped carbon being factored in, a pronounced enhancement is also seen for the performance of NVP. For example, a flowerlike N,B codoped carbon-coated NVP composite delivers a low capacity fading rate of 0.40% that can still be maintained after 2000 cycles at 100 C.[33] Furthermore, we have seen that tremendous strides have been made for NVP as its performance in full cells is getting closer to that of commercial batteries. For example, the full cell based on 3D graphene capped NVP reported by Cao et al. managed to reach an initial Coulombic efficiency as high as 94.3% and sustain a capacity retention of 77.1% over 200 cycles (Figure 5c,d).[39]

4.2. Vanadium Oxides

Vanadium oxides cover a wide range of compositions with different coordination environments and oxidation states, where V_2O_5 and VO_2(B) are particularly interesting, with their rich intercalation chemistry.

Li can be inserted into the layered structure of orthorhombic V_2O_5 at different intercalation depths ($V_2O_5 \leftrightarrow Li_xV_2O_5$), accompanied by a series of phase transitions. Despite its high capacity, the commercialization of V_2O_5 requires further optimization of dimensional and transport parameters. Nanostructuring has been the pioneering effort to overcome the sluggish reaction kinetics of V_2O_5 by capitalizing on the benefit of nanomaterials with rational morphological design.[40] Our latest research has extended this concept to the mass production of V_2O_5 nanostructures, hoping to move that success to industrial applications from an economic standpoint. To achieve this, the ambient dissolution−recrystallization mechanism enables the production of V_2O_5 nanobelts at room temperature at a large scale.[13] From our density functional theory (DFT) calculations, the unusual growth mechanisms of the V_2O_5 nanobelts along the [010] direction differ vastly from the well-accepted calculations where nonlocal correlations are neglected. The excellent performances of these V_2O_5 nanobelts in LIBs and sodium ion batteries (SIBs) are what make us believe its possible commercial viability; for example, specific capacities of 144 and 61 mAh g^{-1} can be achieved at 20 and 10 C for LIBs and SIBs, respectively. Lately, the knowledge gained for the design principle of V_2O_5 was further transferred to the application of V_2O_5 in other battery systems. A V_2O_5 nanorod constructed 3D porous network that was produced in a large scale has been proved to be electrochemically active toward Zn^{2+}.[2] Owing to the unique architecture, this cathode exhibits good performance, sustaining a capacity fading rate of 0.033% over 5000 cycles at a high rate of 10 A g^{-1}. From the mechanistic study based on first-principles calculations, the possible insights that suggest the most favorable intercalation pathway in the [100] channel for Zn^{2+} and a slight shrinkage in the lattice caused by the interaction between the incoming Zn^{2+} and VO_6 units with opposite charge may be useful guidelines in materials design for zinc ion batteries (ZIBs) (Figure 6a,b).

https://dx.doi.org/10.1021/acs.accounts.0c00362
Acc. Chem. Res. XXXX, XXX, XXX−XXX

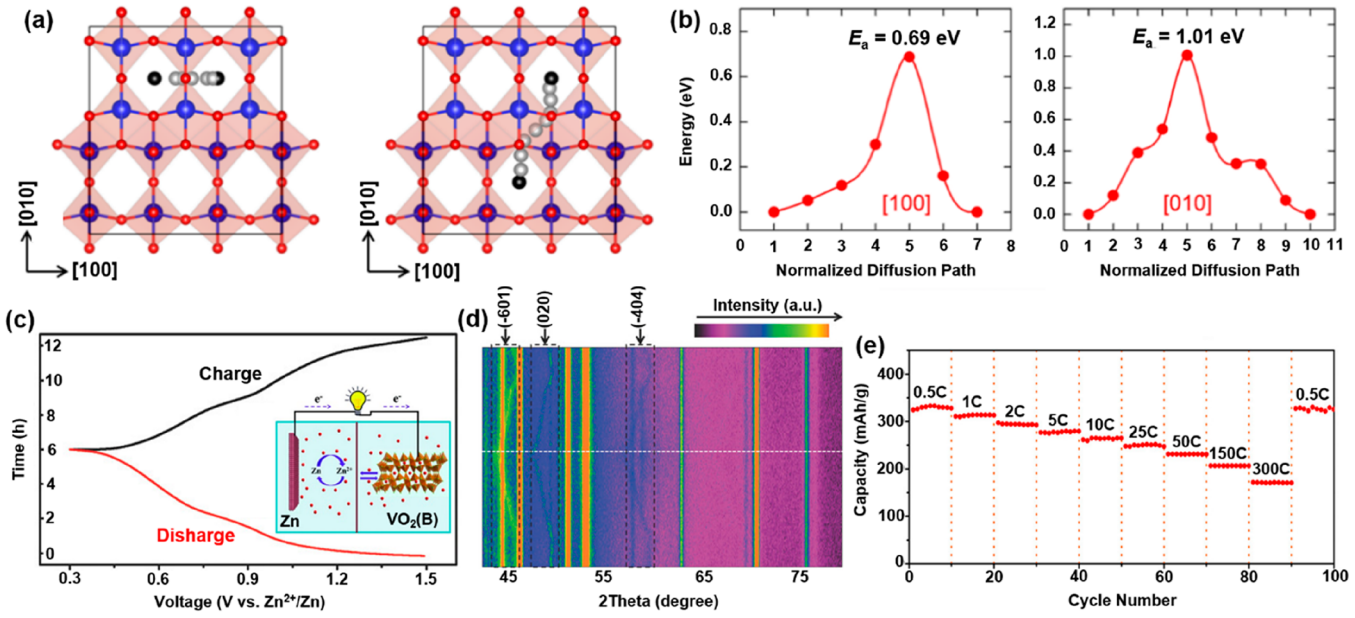

Figure 6. (a) Illustration of the Zn^{2+} diffusion along the [100] and [010] directions in layered V_2O_5 and (b) their corresponding calculated minimum energy paths for Zn^{2+} diffusion. (a, b) Reproduced with permission from ref 2. Copyright 2019 Elsevier. (c) Voltage profile of the VO_2(B) nanofibers at 0.05 C in the Zn//VO_2(B) aqueous battery and (d) the corresponding in situ XRD measurement with 2D contour map. (e) Rate performance of the VO_2(B) nanofibers. (c–e) Reproduced with permission from ref 43. Copyright 2018 Wiley-VCH.

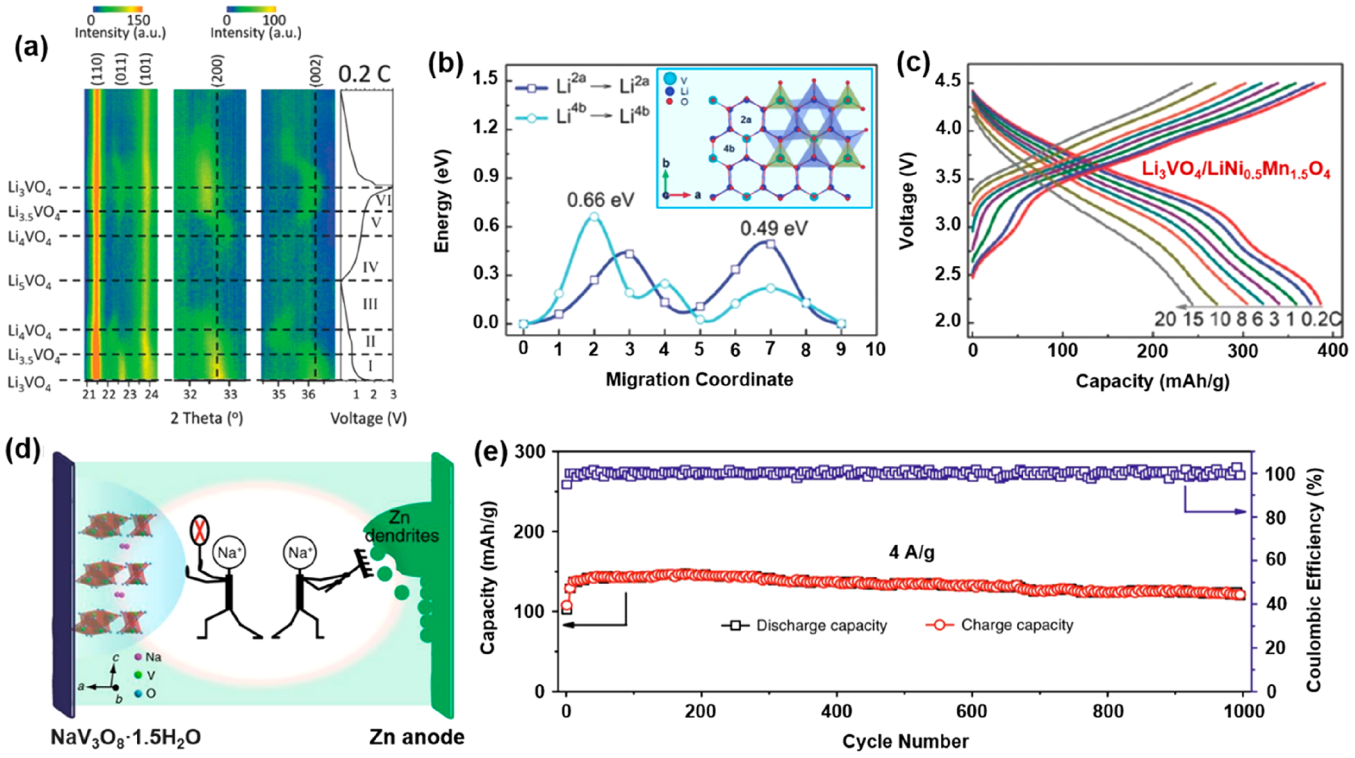

Figure 7. (a) In situ XRD measurement with a 2D contour map of the LVO/C/rGO half-cell at 0.2 C. Reproduced with permission from ref 44. Copyright 2015 Wiley-VCH. (b) Optimized hopping barriers in Li_3VO_4/C (inset: 2 × 2 × 2 supercell of Li_3VO_4 projected along the *c*-axis). Reproduced with permission from ref 9. Copyright 2017 Wiley-VCH. (c) Voltage profiles of the LVO/LNMO full cell at various C rates. Reproduced with permission from ref 3. Copyright 2017 Wiley-VCH. (d) Schematic illustration that shows the role of the Na_2SO_4 additive in suppressing the dissolution of NVO and the formation of Zn dendrites. (e) Cycling performance of the NVO in $ZnSO_4$/Na_2SO_4 electrolyte. (d, e) Reproduced with permission from ref 48. Copyright 2018 Nature Publishing Group.

Among various polymorphic forms of VO_2, monoclinic VO_2(B) with a layered structure is of particular interest. With an increased edge-sharing connectivity of VO_5 square pyramids, VO_2(B) is endowed with better structural stability compared to V_2O_5 as a result of higher resistance to lattice shearing upon cycling.[41] An early study reported by Mai's group has shown the great potential of nanoscroll buffered VO_2(B) in LIBs by demonstrating excellent cycling perform-

https://dx.doi.org/10.1021/acs.accounts.0c00362
Acc. Chem. Res. XXXX, XXX, XXX−XXX

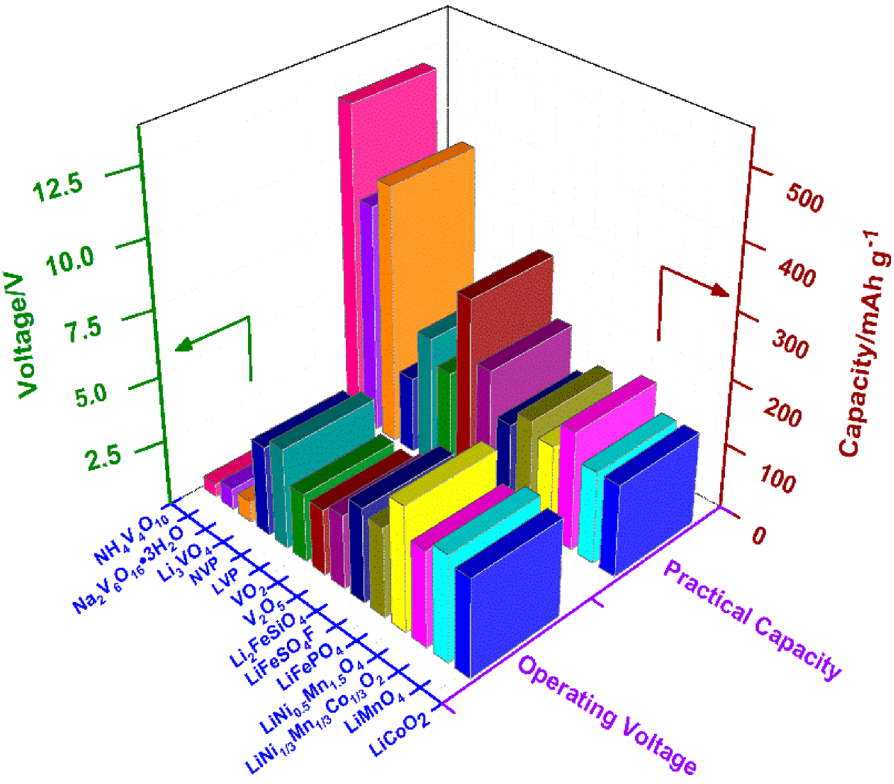

Figure 8. Electrochemical properties of various materials.

ance that shows 82% capacity retention over 1000 cycles.[42] In recent years, the viability of VO_2(B) beyond LIBs has led to a renaissance in research of this material. We have seen the deployment of VO_2(B) in aqueous-based ZIBs, where the charge storage mechanism highly resembles that of LIBs. It has been identified by in situ X-ray diffraction (XRD) study that both of the tunnels parallel to the *b*-axis ((−601) and (−404) facets) or *c*-axis ((020) facet) are the possible transport pathways for Zn^{2+} (de)intercalation (Figure 6c,d).[43] In this study, the VO_2(B) nanofibers deliver discharge capacities as high as 232 and 171 mAh g^{-1} at 50 and 300 C, respectively (Figure 6e). Such promising values can be ascribed to the large transport tunnel of VO_2(B) along with its multiple possible transport routes.

4.3. Vanadates

Li_3VO_4 is an insertion type anode with a 3D lantern-like framework that exhibits many possible sites for Li^+ insertion and high Li^+ mobility in the lattice. A two-electron transition reaction is well-accepted as the intercalation mechanism of Li_3VO_4 upon lithiation (theoretical capacity of 394 mAh g^{-1}), despite new perspectives on the insertion of a maximum of 3 mol Li^+ emerging as the measured capacity exceeding the theoretical value.[44,45] Ongoing research focuses on improving the electronic conductivity of Li_3VO_4, where several research groups have hybridized and doped Li_3VO_4 with foreign substances for modulation of properties. For example, along with the highly reversible (de)intercalation reaction observed via the in situ XRD study (Figure 7a), the electrochemical performance of Li_3VO_4 was further enhanced after modification with carbonaceous materials.[44] The novel insights into the role of hybridization and surface chemistry on the charge storage properties of Li_3VO_4 were further harnessed for the design of a novel Li_3VO_4 in our later study.[9] The mechanistic study carried out by DFT calculation revealed that Li^+ prefers to travel along path 2a rather than path 4a due to the lower energy barrier for diffusion (Figure 7b). Moreover, we also attempted to optimize them through carbon coating and the construction of secondary structures. The N-doped carbon-encapsulated Li_3VO_4 nanowires show excellent power capability, where a capacity of 203 mAh g^{-1} (55% of the capacity obtained at 1 A g^{-1}) can still be maintained at 20 A g^{-1}. Furthermore, when the carbon-coated Li_3VO_4 spheres were coupled with a $LiNi_{0.5}Mn_{1.5}O_4$ cathode in a full cell, they exhibits exceptional rate performance, where 63% capacity obtained at 0.2 C can still be retained under a 10-fold increase in current density (Figure 7c).[3]

Layered vanadate, $Na_2V_6O_{16}\cdot 3H_2O$, consisting of Na^+ and water molecules sandwiched between V_3O_8 layers is suitable for facile intercalation of multivalent ions and is highly compatible with aqueous-based electrolytes. We are particularly interested in aqueous-based batteries, owing to their advantages over organic systems in the aspects of cost-effectiveness, safety features, and power density. In fact, our first few research works on $Na_2V_6O_{16}\cdot 3H_2O$ in aqueous-based ZIBs were motivated by the fast ion transport and better operational feasibility of the aqueous systems, which can be a cost-effective solution for large-scale applications in the long run. Inspired by the study of Mai's group that unraveled the intercalation mechanism of Zn^{2+} in $Na_2V_6O_{16}\cdot 3H_2O$,[46] we further worked through the sluggish charge transfer kinetics and structural instability of $Na_2V_6O_{16}\cdot 3H_2O$ by the nanoscale morphology and pillaring effect of interlayer metal ions as well as structural water.[47] These favorable structural features act in concert to enable a good rate and cycling performance. In a full cell developed by Niu's group, they proved that the $NaV_3O_8\cdot 1.5H_2O$ nanobelts are capable of achieving a high energy

https://dx.doi.org/10.1021/acs.accounts.0c00362
Acc. Chem. Res. XXXX, XXX, XXX−XXX

density of 300 Wh kg^{-1}, on top of a high capacity retention of 82% after 1000 cycles at 4 A g^{-1} (Figure 7d).[48]

Conclusions from the aforementioned studies can be extended beyond $Na_2V_6O_{16}$. It is possible to identify that structural features, such as a large interlayer spacing, a robust charge transport framework, and accessibility of redox active sites, are the parameters that can be tuned to maximize the performance. This has driven our investigation of $NH_4V_4O_{10}$ with ample structural similarity with LiV_3O_8 for ZIBs.[49] When the $NH_4V_4O_{10}$ nanobelts with a 3D flowerlike architecture were assembled on a quasi-solid-state ZIB, the cell stabilized at 378 mAh g^{-1} with almost 100% Coulombic efficiency after 50 cycles. Aside from experimental investigations through ex situ techniques, theoretical calculations were also carried to answer those unresolved queries regarding the intercalation mechanism of layered $Na_2V_6O_{16}\cdot 3H_2O$. The extended step has established a theory that can be applied to illustrate the working mechanism and predict the performance by taking into consideration the preferential diffusion of Zn^{2+} ions along the [010] direction within the interlayer space.

5. CONCLUSION AND PERSPECTIVES

Tunable electrochemical behaviors accompanied by a rich redox chemistry in V-compounds have made them the focus of interest in various battery systems spanning from monovalent to multivalent-ion batteries, where their electrochemical properties are compared with other conventional materials in Figure 8. However, their viability is still being questioned from the perspective of cost and toxicity. Therefore, further studies are still required to fully understand the toxicology as well as the biological and pharmacological activity of vanadium. In addition, the high cost of vanadium will likely to add up to a hefty production cost that might dictate against their use in large-scale applications. The applicability of V-compounds is also challenged by their slow reaction kinetics arising from the low conductivity. Thus, amelioration of the existing techniques to further modify the intrinsic properties of V-compounds is the missing piece to make them more competitive for commercial applications. In the following paragraph, we highlight some of the research directions, in our opinion, that are essential for the further advancement of vanadium-based electrodes.

The confluence of material synthesis, real-time characterizations, and computational simulations will be the way of the future for research of V-compounds. Recent advances in nanotechnology are making V-compounds more synthetically accessible with nanoscale precision. However, careful attention should be directed toward the handling of the complexity of materials design as the disappearance of one disadvantage might be accompanied by several other issues for nanostructured V-compounds (e.g., unwanted parasitic reactions, unstable SEI formation, and severe aggregation). A better understanding of the charge storage and failure mechanisms transforms our ability to design better V-compounds. Nevertheless, the central to challenge is that this can barely be resolved by experimental means. What is needed is real-time monitoring platforms capable of providing simultaneous information on the compositional and structural evolutions of V-compounds during battery operation. Under certain circumstances where current characterization techniques are short of being satisfactory to provide adequate resolution to the identification of the short-lived intermediates and elucidation of the reaction mechanism at a detailed level, we might need to resort to computational methods, such as DFT calculations and machine learning, to supply the missing information that is inaccessible by experiments.

Given the commitment of vanadium-based electrodes, a question arises: What does the future hold for the vanadium-based electrode? We think the potential impact that V-compounds may have on the future of battery technology will be huge, where the findings may pave the way for innovation in this field. However, we do realize that V-compounds still require more advanced designs and strategies to convert this game-changing innovation into a commercially embedded technology, which is the direction that we are keen to work through down the road.

AUTHOR INFORMATION

Corresponding Authors

Yan Yu − *Hefei National Laboratory for Physical Sciences at the Microscale, Department of Materials Science and Engineering, CAS Key Laboratory of Materials for Energy Conversion, University of Science and Technology of China, Hefei, Anhui 230026, China; Dalian National Laboratory for Clean Energy (DNL), Chinese Academy of Sciences (CAS), Dalian 116023, China;* orcid.org/0000-0002-3685-7773; Email: yanyumse@ustc.edu.cn

Xianhong Rui − *Guangzhou Key Laboratory of Low-Dimensional Materials and Energy Storage Devices, School of Materials and Energy, Guangdong University of Technology, Guangzhou 510006, China;* orcid.org/0000-0003-1125-0905; Email: xhrui@gdut.edu.cn

Authors

Shipeng Zhang − *State Key Lab Incubation Base of Photoelectric Technology and Functional Materials, International Collaborative Center on Photoelectric Technology and Nano Functional Materials, Institute of Photonics and Photon-Technology, Northwest University, Xi'an 710069, China; Hefei National Laboratory for Physical Sciences at the Microscale, Department of Materials Science and Engineering, CAS Key Laboratory of Materials for Energy Conversion, University of Science and Technology of China, Hefei, Anhui 230026, China*

Huiteng Tan − *Guangzhou Key Laboratory of Low-Dimensional Materials and Energy Storage Devices, School of Materials and Energy, Guangdong University of Technology, Guangzhou 510006, China*

Complete contact information is available at: https://pubs.acs.org/10.1021/acs.accounts.0c00362

Author Contributions

$^{\perp}$S.Z. and H.T. contributed equally to this work.

Notes

The authors declare no competing financial interest.

Biographies

Shipeng Zhang is a Ph.D. graduate student at Northwest University, China. His research interests focus on the development of novel energy storage materials.

Huiteng Tan received her Ph.D. degree from Nanyang Technological University in 2015. Her research interests focus on developing advanced electrode materials for energy storage systems.

https://dx.doi.org/10.1021/acs.accounts.0c00362
Acc. Chem. Res. XXXX, XXX, XXX−XXX

Xianhong Rui is a professor of the School of Materials and Energy at Guangdong University of Technology, China. He received his Ph.D. degree from Nanyang Technological University in 2014. His research interests mainly focus on the design and fabrication of advanced electrode materials (especially V-compounds) for energy conversion and storage.

Yan Yu is a professor of material science at the University of Science and Technology of China (USTC). She received her Ph.D. in material science at USTC in 2006. Her current research interests mainly include the design of novel nanomaterials for clean energy, especially for batteries and the fundamental science of energy-storage systems.

■ ACKNOWLEDGMENTS

The authors gratefully acknowledge the National Key R&D Research Program of China (Grant No. 2018YFB0905400), National Natural Science Foundation of China (Grant Nos. 51925207, 21606003, 51972067, 51802044, 51872277, and U1910210), the Fundamental Research Funds for the Central Universities (WK2060140026), the DNL cooperation Fund, CAS (DNL180310), and Guangdong Natural Science Funds for Distinguished Young Scholar (Grant No. 2019B151502039).

■ REFERENCES

(1) Rui, X.; Sun, W.; Wu, C.; Yu, Y.; Yan, Q. An Advanced Sodium-Ion Battery Composed of Carbon Coated $Na_3V_2(PO_4)_3$ in a Porous Graphene Network. *Adv. Mater.* **2015**, *27*, 6670−6676.
(2) Chen, D.; Rui, X.; Zhang, Q.; Geng, H.; Gan, L.; Zhang, W.; Li, C.; Huang, S.; Yu, Y. Persistent Zinc-Ion Storage in Mass-Produced V_2O_5 Architectures. *Nano Energy* **2019**, *60*, 171−178.
(3) Shen, L.; Chen, S.; Maier, J.; Yu, Y. Carbon-Coated Li_3VO_4 Spheres as Constituents of an Advanced Anode Material for High-Rate Long-Life Lithium-Ion Batteries. *Adv. Mater.* **2017**, *29*, 1701571.
(4) Ding, Y.-L.; Wen, Y.; Wu, C.; van Aken, P. A.; Maier, J.; Yu, Y. 3D V_6O_{13} Nanotextiles Assembled from Interconnected Nanogrooves as Cathode Materials for High-Energy Lithium Ion Batteries. *Nano Lett.* **2015**, *15*, 1388−1394.
(5) Cambaz, M. A.; Vinayan, B. P.; Pervez, S. A.; Johnsen, R. E.; Geßwein, H.; Guda, A. A.; Rusalev, Y. V.; Kinyanjui, M. K.; Kaiser, U.; Fichtner, M. Suppressing Dissolution of Vanadium from Cation-Disordered $Li_{2-x}VO_2F$ via a Concentrated Electrolyte Approach. *Chem. Mater.* **2019**, *31*, 7941−7950.
(6) Wagemaker, M.; Mulder, F. M. Properties and Promises of Nanosized Insertion Materials for Li-Ion Batteries. *Acc. Chem. Res.* **2013**, *46*, 1206−1215.
(7) Van der Ven, A.; Bhattacharya, J.; Belak, A. A. Understanding Li Diffusion in Li-Intercalation Compounds. *Acc. Chem. Res.* **2013**, *46*, 1216−1225.
(8) Rui, X. H.; Ding, N.; Liu, J.; Li, C.; Chen, C. H. Analysis of the chemical diffusion coefficient of lithium ions in $Li_3V_2(PO_4)_3$ cathode material. *Electrochim. Acta* **2010**, *55*, 2384−2390.
(9) Shen, L.; Lv, H.; Chen, S.; Kopold, P.; van Aken, P. A.; Wu, X.; Maier, J.; Yu, Y. Peapod-like Li_3VO_4/N-Doped Carbon Nanowires with Pseudocapacitive Properties as Advanced Materials for High-Energy Lithium-Ion Capacitors. *Adv. Mater.* **2017**, *29*, 1700142.
(10) Zhang, Z.; Chen, Z.; Mai, Z.; Peng, K.; Deng, Q.; Bayaguud, A.; Zhao, P.; Fu, Y.; Yu, Y.; Zhu, C. Toward High Power-High Energy Sodium Cathodes: A Case Study of Bicontinuous Ordered Network of 3D Porous $Na_3(VO)_2(PO4)_2F$/rGO with Pseudocapacitance Effect. *Small* **2019**, *15*, 1900356.
(11) Winter, M.; Brodd, R. J. What Are Batteries, Fuel Cells, and Supercapacitors? *Chem. Rev.* **2004**, *104*, 4245−4270.
(12) Tang, Y.; Zhang, Y.; Li, W.; Ma, B.; Chen, X. Rational Material Design for Ultrafast Rechargeable Lithium-Ion Batteries. *Chem. Soc. Rev.* **2015**, *44*, 5926−5940.
(13) Rui, X.; Tang, Y.; Malyi, O. I.; Gusak, A.; Zhang, Y.; Niu, Z.; Tan, H. T.; Persson, C.; Chen, X.; Chen, Z.; Yan, Q. Ambient Dissolution−Recrystallization towards Large-Scale Preparation of V_2O_5 Nanobelts for High-Energy Battery Applications. *Nano Energy* **2016**, *22*, 583−593.
(14) Tan, H. T.; Rui, X.; Sun, W.; Yan, Q.; Lim, T. M. Vanadium-Based Nanostructure Materials for Secondary Lithium Battery Applications. *Nanoscale* **2015**, *7*, 14595−14607.
(15) Rui, X.; Lu, Z.; Yu, H.; Yang, D.; Hng, H. H.; Lim, T. M.; Yan, Q. Ultrathin V_2O_5 Nanosheet Cathodes: Realizing Ultrafast Reversible Lithium Storage. *Nanoscale* **2013**, *5*, 556−560.
(16) Yu, K.; Pan, X.; Zhang, G.; Liao, X.; Zhou, X.; Yan, M.; Xu, L.; Mai, L. Nanowires in Energy Storage Devices: Structures, Synthesis, and Applications. *Adv. Energy Mater.* **2018**, *8*, 1802369.
(17) Chen, D.; Tan, H.; Rui, X.; Zhang, Q.; Feng, Y.; Geng, H.; Li, C.; Huang, S.; Yu, Y. Oxyvanite V_3O_5: A New Intercalation-Type Anode for Lithium-Ion Battery. *InfoMat* **2019**, *1*, 251−259.
(18) Gogotsi, Y.; Penner, R. M. Energy Storage in Nanomaterials−Capacitive, Pseudocapacitive, or Battery-like? *ACS Nano* **2018**, *12*, 2081−2083.
(19) Li, Q.; Chen, D.; Tan, H.; Zhang, X.; Rui, X.; Yu, Y. 3D Porous V_2O_5 Architectures for High-Rate Lithium Storage. *J. Energy Chem.* **2020**, *40*, 15−21.
(20) Shen, L.; Wang, Y.; Wu, F.; Moudrakovski, I.; van Aken, P. A.; Maier, J.; Yu, Y. Hierarchical Metal Sulfide/Carbon Spheres: A Generalized Synthesis and High Sodium-Storage Performance. *Angew. Chem., Int. Ed.* **2019**, *58*, 7238−7243.
(21) Muldoon, J.; Bucur, C. B.; Gregory, T. Quest for Nonaqueous Multivalent Secondary Batteries: Magnesium and Beyond. *Chem. Rev.* **2014**, *114*, 11683−11720.
(22) Kundu, D.; Adams, B. D.; Duffort, V.; Vajargah, S. H.; Nazar, L. F. A High-Capacity and Long-Life Aqueous Rechargeable Zinc Battery Using a Metal Oxide Intercalation Cathode. *Nat. Energy* **2016**, *1*, 16119.
(23) Xia, C.; Guo, J.; Li, P.; Zhang, X.; Alshareef, H. N. Highly Stable Aqueous Zinc-Ion Storage Using a Layered Calcium Vanadium Oxide Bronze Cathode. *Angew. Chem., Int. Ed.* **2018**, *57*, 3943−3948.
(24) Liu, C.; Massé, R.; Nan, X.; Cao, G. A Promising Cathode for Li-Ion Batteries: $Li_3V_2(PO_4)_3$. *Energy Storage Mater.* **2016**, *4*, 15−58.
(25) Kulish, V. V.; Malyi, O. I.; Ng, M.-F.; Chen, Z.; Manzhos, S.; Wu, P. Controlling Na Diffusion by Rational Design of Si-Based Layered Architectures. *Phys. Chem. Chem. Phys.* **2014**, *16*, 4260−4267.
(26) Liu, C.; Neale, Z.; Zheng, J.; Jia, X.; Huang, J.; Yan, M.; Tian, M.; Wang, M.; Yang, J.; Cao, G. Expanded Hydrated Vanadate For High-Performance Aqueous Zinc-Ion Batteries. *Energy Environ. Sci.* **2019**, *12*, 2273−2285.
(27) Sun, C.; Rajasekhara, S.; Dong, Y.; Goodenough, J. B. Hydrothermal Synthesis and Electrochemical Properties of $Li_3V_2(PO_4)_3$/C-Based Composites for Lithium-Ion Batteries. *ACS Appl. Mater. Interfaces* **2011**, *3*, 3772−3776.
(28) Zhang, C.; Liu, C.; Nan, X.; Song, H.; Liu, Y.; Zhang, C.; Cao, G. Hollow−Cuboid Li_3VO_4/C as High-Performance Anodes for Lithium-Ion Batteries. *ACS Appl. Mater. Interfaces* **2016**, *8*, 680−688.
(29) Rui, X. H.; Li, C.; Liu, J.; Cheng, T.; Chen, C. H. The $Li_3V_2(PO_4)_3$/C Composites with High-Rate Capability Prepared by a Maltose-Based Sol−Gel Route. *Electrochim. Acta* **2010**, *55*, 6761−6767.
(30) Yao, Y.; Jiang, Y.; Yang, H.; Sun, X.; Yu, Y. $Na_3V_2(PO_4)_3$ Coated by N-Doped Carbon from Ionic Liquid as Cathode Materials for High Rate and Long-Life Na-Ion Batteries. *Nanoscale* **2017**, *9*, 10880−10885.
(31) Kong, D.; Li, X.; Zhang, Y.; Hai, X.; Wang, B.; Qiu, X.; Song, Q.; Yang, Q.-H.; Zhi, L. Encapsulating V_2O_5 into Carbon Nanotubes Enables the Synthesis of Flexible High-Performance Lithium Ion Batteries. *Energy Environ. Sci.* **2016**, *9*, 906−911.
(32) Ren, W.; Zheng, Z.; Xu, C.; Niu, C.; Wei, Q.; An, Q.; Zhao, K.; Yan, M.; Qin, M.; Mai, L. Self-Sacrificed Synthesis of Three-Dimensional $Na_3V_2(PO_4)_3$ Nanofiber Network for High-Rate Sodium−Ion Full Batteries. *Nano Energy* **2016**, *25*, 145−153.

https://dx.doi.org/10.1021/acs.accounts.0c00362
Acc. Chem. Res. XXXX, XXX, XXX−XXX

(33) Jiang, Y.; Zhou, X.; Li, D.; Cheng, X.; Liu, F.; Yu, Y. Highly Reversible Na Storage in $Na_3V_2(PO_4)_3$ by Optimizing Nanostructure and Rational Surface Engineering. *Adv. Energy Mater.* **2018**, *8*, 1800068.
(34) Tan, H.; Xu, L.; Geng, H.; Rui, X.; Li, C.; Huang, S. Nanostructured $Li_3V_2(PO_4)_3$ Cathodes. *Small* **2018**, *14*, 1800567.
(35) Zhang, X.; Kühnel, R.-S.; Hu, H.; Eder, D.; Balducci, A. Going Nano with Protic Ionic Liquids—the Synthesis of Carbon Coated $Li_3V_2(PO_4)_3$ Nanoparticles Encapsulated in a Carbon Matrix for High Power Lithium-Ion Batteries. *Nano Energy* **2015**, *12*, 207−214.
(36) Luo, Y.; Xu, X.; Zhang, Y.; Pi, Y.; Zhao, Y.; Tian, X.; An, Q.; Wei, Q.; Mai, L. Hierarchical Carbon Decorated $Li_3V_2(PO_4)_3$ as a Bicontinuous Cathode with High-Rate Capability and Broad Temperature Adaptability. *Adv. Energy Mater.* **2014**, *4*, 1400107.
(37) Zhou, Y.; Rui, X.; Sun, W.; Xu, Z.; Zhou, Y.; Ng, W. J.; Yan, Q.; Fong, E. Biochemistry-Enabled 3D Foams for Ultrafast Battery Cathodes. *ACS Nano* **2015**, *9*, 4628−4635.
(38) Zhu, C.; Song, K.; van Aken, P. A.; Maier, J.; Yu, Y. Carbon-Coated $Na_3V_2(PO_4)_3$ Embedded in Porous Carbon Matrix: An Ultrafast Na-Storage Cathode with the Potential of Outperforming Li Cathodes. *Nano Lett.* **2014**, *14*, 2175−2180.
(39) Cao, X.; Pan, A.; Liu, S.; Zhou, J.; Li, S.; Cao, G.; Liu, J.; Liang, S. Chemical Synthesis of 3D Graphene-Like Cages for Sodium-Ion Batteries Applications. *Adv. Energy Mater.* **2017**, *7*, 1700797.
(40) Xu, X.; Xiong, F.; Meng, J.; Wang, X.; Niu, C.; An, Q.; Mai, L. Vanadium-Based Nanomaterials: A Promising Family for Emerging Metal-Ion Batteries. *Adv. Funct. Mater.* **2020**, *30*, 1904398.
(41) Rui, X.; Sim, D.; Xu, C.; Liu, W.; Tan, H.; Wong, K.; Hng, H. H.; Lim, T. M.; Yan, Q. One-pot synthesis of carbon-coated VO_2(B) nanobelts for high-rate lithium storage. *RSC Adv.* **2012**, *2*, 1174−1180.
(42) Mai, L.; Wei, Q.; An, Q.; Tian, X.; Zhao, Y.; Xu, X.; Xu, L.; Chang, L.; Zhang, Q. Nanoscroll Buffered Hybrid Nanostructural VO_2(B) Cathodes for High-Rate and Long-Life Lithium Storage. *Adv. Mater.* **2013**, *25*, 2969−2973.
(43) Ding, J.; Du, Z.; Gu, L.; Li, B.; Wang, L.; Wang, S.; Gong, Y.; Yang, S. Ultrafast Zn^{2+} Intercalation and Deintercalation in Vanadium Dioxide. *Adv. Mater.* **2018**, *30*, 1800762.
(44) Li, Q.; Wei, Q.; Sheng, J.; Yan, M.; Zhou, L.; Luo, W.; Sun, R.; Mai, L. Mesoporous Li_3VO_4/C Submicron-Ellipsoids Supported on Reduced Graphene Oxide as Practical Anode for High-Power Lithium-Ion Batteries. *Adv. Sci.* **2015**, *2*, 1500284.
(45) Liang, Z.; Lin, Z.; Zhao, Y.; Dong, Y.; Kuang, Q.; Lin, X.; Liu, X.; Yan, D. New Understanding of Li_3VO_4/C as Potential Anode for Li-Ion Batteries: Preparation, Structure Characterization and Lithium Insertion Mechanism. *J. Power Sources* **2015**, *274*, 345−354.
(46) Hu, P.; Zhu, T.; Wang, X.; Wei, X.; Yan, M.; Li, J.; Luo, W.; Yang, W.; Zhang, W.; Zhou, L.; Zhou, Z.; Mai, L. Highly Durable $Na_2V_6O_{16}$·$1.63H_2O$ Nanowire Cathode for Aqueous Zinc-Ion Battery. *Nano Lett.* **2018**, *18*, 1758−1763.
(47) Tan, H.; Chen, D.; Liu, W.; Liu, C.; Lu, B.; Rui, X.; Yan, Q. Free-Standing Hydrated Sodium Vanadate Papers for High-Stability Zinc-Ion Batteries. *Batteries & Supercaps* **2020**, *3*, 254−260.
(48) Wan, F.; Zhang, L.; Dai, X.; Wang, X.; Niu, Z.; Chen, J. Aqueous Rechargeable Zinc/Sodium Vanadate Batteries with Enhanced Performance from Simultaneous Insertion of Dual Carriers. *Nat. Commun.* **2018**, *9*, 1656.
(49) Li, Q.; Rui, X.; Chen, D.; Feng, Y.; Xiao, N.; Gan, L.; Zhang, Q.; Yu, Y.; Huang, S. A High Capacity Ammonium Vanadate Cathode for Zinc-Ion Battery. *Nano-Micro Lett.* **2020**, *12*, 67.

https://dx.doi.org/10.1021/acs.accounts.0c00362
Acc. Chem. Res. XXXX, XXX, XXX−XXX